FOCUS ON BIOTECHNOLOGY

Fundamentals of Cell Immobilisation Biotechnology

Edited by
Viktor Nedović and Ronnie Willaert

Series Editors: Marcel Hofman and Jozef Anné

Kluwer Academic Publishers

IMMOBILIZATION OF CELLS AND ENZYMES USING ELECTROSTATIC DROPLET GENERATION

BRANKO M. BUGARSKI[1], BOJANA OBRADOVIC[1], VIKTOR A. NEDOVIC[2] AND DENIS PONCELET[3]

[1]Department of Chemical Engineering, Faculty of Technology and Metallurgy, University of Belgrade, Karnegijeva 4, 11000 Belgrade, Yugoslavia – Fax: + 381113370472 – Email: branko@elab.tmf.bg.ac.yu

[2]Department of Food Technology and Biochemistry, Faculty of Agriculture, University of Belgrade, Nemanjina 6, 11081 Belgrade-Zemun, Yugoslavia – Fax: +38111193659 – Email: vnedovic@eunet.yu

[3]ENITIAA, Rue de la Géraudiere, BP 82 225, Nantes, 44322, France – Fax: +33 2 51 78 54 67 – Email: poncelet@enitiaa-nantes.fr

Abstract

Selection of support material and method of immobilization is made by weighing the various characteristics and required features of the cell/enzyme application against the properties and limitations of the combined immobilization and support. A number of practical aspects should be considered before embarking on experimental work to ensure that the final immobilized cell or enzyme preparation is fit for the planned purpose or application to operate at optimum effectiveness. The mechanism of alginate droplet formation as well as experimental parameters for producing small hydro gel beads using an electrostatic droplet generator was investigated. It was found that microbead size was a function of needle diameter, charge arrangement (*i.e.* electrode geometry and spacing) and strength of the electric field. The process of alginate droplet formation under the influence of electrostatic forces was assessed with an image analysis/video system and revealed distinct stages; after a voltage was applied the liquid meniscus at the needle tip was distorted from a spherical shape into an inverted cone-like shape. Alginate solution flowed into this cone at an increasing rate causing formation of a neck-like filament. When this filament broke away, producing small droplets, the meniscus relaxed back to a spherical shape until flow of the alginate caused the process to start again. Various cells suspensions and enzymes were subjected to a high voltage immobilization process in order to assess the effects of electric fields on animal cell viability and enzyme activity. There was no detectable loss in cell viability or enzyme activity after the voltage was applied.

V. Nedović and R. Willaert (eds.), Fundamentals of Cell Immobilisation Biotechnology, 277-294.
© 2004 *Kluwer Academic Publishers. Printed in the Netherlands.*

1. Introduction

Immobilization of cells and enzymes by physical entrapment in polymer hydrogels and insoluble interpolyelectrolyte complexes is widely used in bioencapsulation technology [1]. A common procedure for producing gel microbeads involves dispersing a polymer solution into a hardening (collecting) solution using air jet extrusion technology [2-4]. One of the major concerns in cell and bioactive agent immobilization has been the production of small microbeads to minimize the mass transfer resistance associated with large diameter beads (>1000 μm). Different immobilization systems such as: gel-forming proteins (gelatin), polysaccharides (agar, alginates, κ-carrageenan) and synthetic polymers (polyacrylamide) are used to obtain hydrogel beads. Bivalent Ca^{2+} commonly produces the ionic cross-linking in a hardening solution.

Research and development work has provided a bewildering array of support materials and methods for immobilization. Much of the expansion may be attributed to attempts to provide specific improvements for a given application. The growing interest in the field of cell immobilization has led to the development of numerous techniques such as dripping [5,6], emulsification or coacervation [7,8,9], rotating disc atomization [10,11], air jet [12,13], atomization [14], electrostatic dripping [15,16], mechanical cutting [17], and the vibrating nozzle technique [18,19,20], all of which suffer from certain limitations. No technique allows for the simultaneous production of beads with a narrow size distribution under high production rate and in completely sterile conditions with ability to scale-up [21].

However, electrostatic extrusion can be used to produce beads less than 300 microns with a narrow size distribution with possibility to operate under sterile conditions. Also, a modification of geometry set-up system, in the form of a multi-needle device, showed that it is possible to continuously produce relatively uniform microbeads at a high processing capacity.

Acceleration of the droplet formation process and significant decrease of droplet size may be realized by applying electrical potential to polymer solutions and this idea is used in electrostatic droplet generation [22,23]. The basic concept behind this application involves the electrostatic force, which acts to disrupt a liquid surface to form a charged stream of fine droplets. The effect of electrostatic forces on mechanically atomized liquid droplets was first studied in detail by Lord Rayleigh [24] who investigated the hydrodynamic stability of a jet of liquid with and without an applied electric field.

When a liquid is subjected to an electric field, a charge is induced on the surface of the liquid. Mutual charge repulsion results in an outwardly directed force. Under suitable conditions, for example extrusion of a liquid through a needle, the electrostatic pressure at the surface forces the liquid drop into a cone shape. Surplus charge is ejected by the emission of charged droplets from the tip of the liquid. The emission process depends on factors such as the needle diameter, distance from the collecting solution and applied voltage [25,26]. Under most circumstances, the electrical spraying process is random and irregular resulting in drops of varying size and charge, emitted from the capillary tip over a wide range of angles. However, when the electrostatic generator configuration is adjusted for liquid pressure, applied voltage, electrode spacing and charge polarity, the spraying process can become quite regular and periodic.

Surprisingly, few attempts have been made in the application of electric fields for the production of micron size polymer beads for cell immobilization.

The primary objective of our work was to investigate the mechanism of droplet formation as well as the experimental parameters, which are critical for producing very small polymer microbeads (*i.e.*, less than 300 μm diameter) using an electrostatic droplet generator. Parameters such as applied voltage, needle size, polymer concentration, and electrode spacing and geometry were assessed. The study was limited to two cases where a positively charged vertically mounted needle and a parallel plate electrode setup were used to extrude alginate solutions at a low constant flow rate. Video and image analysis was performed to reveal details of the mechanism of droplet formation under the influence of an electrostatic field.

A variety of cells were immobilized using electrostatic droplet generation in order 1) to verify that technique was not harmful to the cells and that viability of cells did not change, and 2) to show that cells immobilized using this set-up can grow, multiply and produce normally, which means that cells are not affected by suggested method. Electrostatic droplet generation was used for immobilization of: hybridomas [1,27], insect cells [1,28], islets of Langerhans [1,29,30], parathyroid cells [31] and brewing yeast cells [32-34]. Recently the electrostatic spraying technique was used for enzyme immobilization and production of lipase-alginate beads [35].

2. Experimental studies

2.1. DROPLET FORMATION USING ELECTROSTATIC DROPLET GENERATION

Spherical droplets were formed by a syringe pump (Razel, Scientific Instruments, Stanford, CT, USA) / electrostatic droplet generator which extruded the polymer through a 22 or 26 gauge needle (H80763, H80429, Chromatographic Specialties Inc., Brockville, Canada). As the liquid was forced out of the end of the needle by the syringe pump the droplets were pulled off by the action of gravitational and electrostatic forces. The needle tip was mounted 2.5, 3.5 and 4.8 cm above the 1.5% $CaCl_2$ hardening solution (BDH, Toronto, Canada). The potential difference was controlled by a voltage power supply (Model 30R, Bertan Associates, Inc, N.Y.) with a maximum current of 0.4 mA and variable voltage of 0 to 30 kV (Figure 1).

Our investigation was focused on the effect of charge polarity arrangement, polymer concentration, electrode spacing/geometry and needle size, on average bead diameter. Three types of experiments were carried out in order to determine the optimum conditions for the production of small polymer beads. In the first set-up, a parallel-plate electrode system was employed to produce a uniform electric field in the same direction as that of gravity (Figure 2A). The upper electrode was brought to a positive potential and the polymer droplets were formed at a 90° blunt needle protruding through a small aperture at the centre of the disk electrode. The grounded plate with a hardening solution ($CaCl_2$) had the same dimensions as the upper charged plate.

In the second type of experiments, the effect of a point to plane charge on droplet formation was examined. Namely, the production of charged polymer beads was

accomplished by establishing an electric field between a positively charged needle and a grounded plate containing 1.5% $CaCl_2$ hardening solution (Figure 2B).
Finally, for scale-up purposes a 1.5 litre cylindrical reservoir with twenty needles for the continuous production of polymer beads was designed (Figure 2C). The liquid flow rate was kept constant at 0.7 l/h (36 ml/h per needle) by adjusting the air pressure head above the polymer solution. A ground collecting plate of $CaCl_2$ solution was placed 2.5 cm below the needles. Twenty stainless steel needles (22 gauge) 1.2 cm radially apart were connected to the cylindrical reservoir containing 1 litre of polymer solution and then attached to the high potential unit.

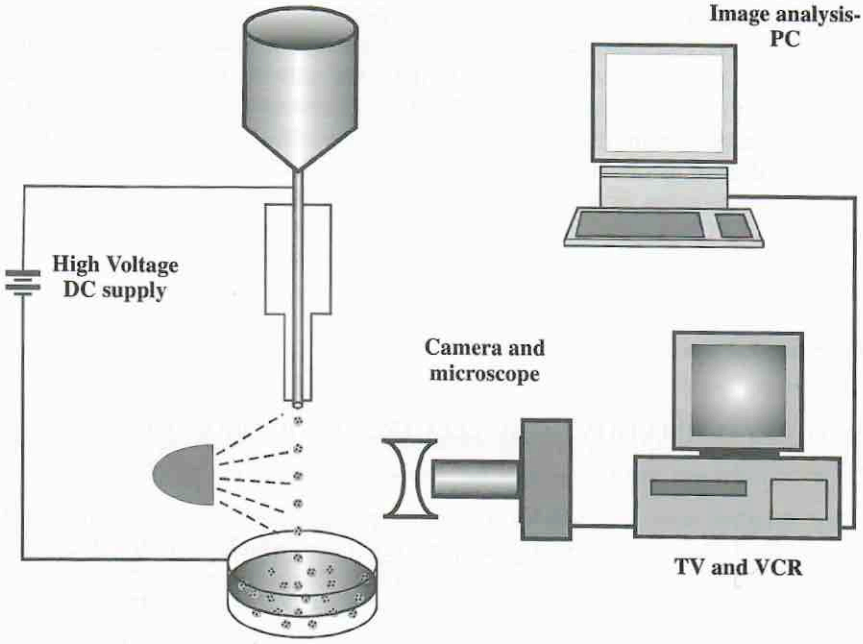

Figure 1. Schematic diagram of the experimental set-up.

2.2. ANALYSIS OF THE DROPLET FORMATION USING IMAGE ANALYSIS

The image analysis system consisted of a video camera (Panasonic Digital 51000m) video Adapter (Sony Trinitrom PVM 1342Q) and VHS recorder (Panasonic NV8950), and the results were analyzed with java version 1.3 software for image analysis (Jandel scientific, CA). For close-up studies of droplet formation, the video was connected to a microscope lens (Olympus SYH, Japan). Droplet images were frozen under a strobe light (Stobatac, GRC, MA) at defined frequencies between 50 and 400 Hz.

2.3. DETERMINATION OF MICROBEAD SIZE DISTRIBUTION

Volumetric (volume of micro spheres in each diameter class) and volumetric cumulative bead size distributions were determined by laser light scattering using a 2602-LC particle analyzer (Malvern Instruments) and HR 850 (Cilas-Alcatel) according to a log-normal distribution model. The mean diameter d_{50} was evaluated at 50% of the cumulative volume fraction. Resolution of the size has been evaluated to less than 10% by replications of the measurement.

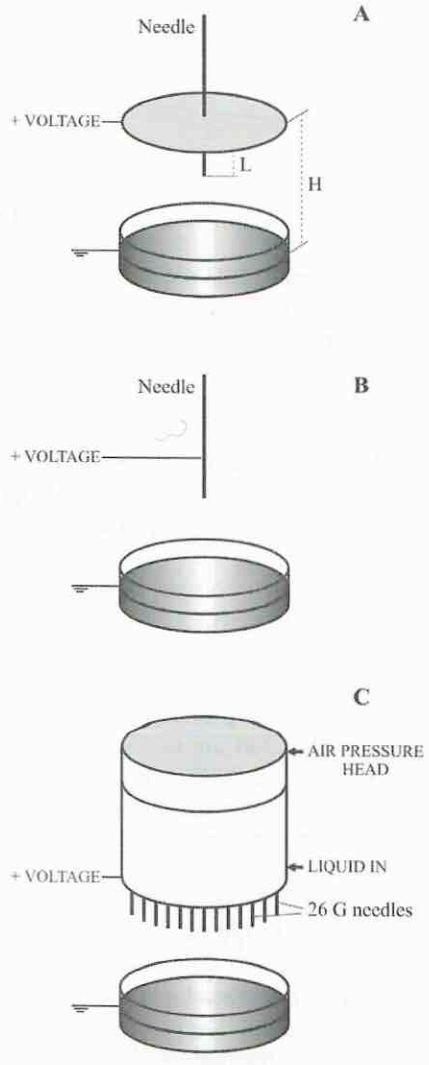

Figure 2. Electrode arrangements: A) Parallel plate set-up with a positively charged plate, B) Positively charged needle, C) Multineedle parallel plate device.

2.4. EXTRUSION OF AN ANIMAL CELL SUSPENSION USING ELECTROSTATIC DROPLET GENERATOR

Animal cell sensitivity directly exposed to a high potential (6-8 kV) was examined by extruding an insect cell (SF-9) suspension using charged needle set-up with a 26 g. needle. The cell viability was assessed by staining the cells with trypan blue dye. The cells were cultured in shake flasks in IPL41 medium prior to extrusion.

To assess cell growth and functional activity as well as the enzyme activity, several types of cells (hybridoma [1,27], insect [1,28], Langerhans islet [1,29,30], yeast [32-34]), and enzymes (lipases [35]) were subjected to immobilization in defined electrostatic field.

3. Results and discussion

3.1. INVESTIGATION OF PARAMETERS AFFECTING MICROBEAD SIZE

In the case of the positively charged needle set-up, the effect of electrode spacing on alginate bead size, produced with a 22 gauge needle, is shown in Figure 3A. The electrode spacing was not found to be significant over the range investigated. For example, at an applied voltage of 6 kV the mean bead size decreased from 530 to 600 μm with a standard deviation of approximately 100 μm, as the electrode spacing decreased from 4.8 to 2.5 cm, respectively. When the applied voltage to the alginate solution was increased to 12 kV, at a distance between needle tip and collecting solution of 4.8 cm, the average bead diameter decreased to 340 μm. Keeping the applied potential constant at 12 kV, but reducing the electrode distance to 2.5 cm, resulted in only a slightly smaller bead size (300 μm).

The relationship between the applied voltage, alginate concentration and droplet diameter was also investigated (Figure 3B,C). When the alginate concentration was decreased from 1.5% to 0.8% the average bead diameter decreased for the most 20%. At the lower polymer concentration the standard deviation decreased, due to a more uniform bead size distribution. For example, at an applied voltage of 5 kV the mean bead diameter decreased from 440 ± 200 μm to 380 ± 80 μm, for the beads prepared with alginate concentrations of 1.5% and 0.8%, respectively.

While the alginate concentration was not found to be a significant parameter, bead diameter could be readily controlled by the needle size and applied voltage (Figure 3B,C). For example at an applied voltage of 4 kV the mean bead diameter was reduced by a factor of 3 from approximately 1600 μm to 500 μm when the needle size was reduced from 22 gauge to 26 gauge. In the case of the 26-gauge needle as the voltage increased above 6 kV, natural harmonic oscillation of the needle was observed. This resulted in bimodal distribution of microbead sizes with a large fraction of 50 μm in diameter.

A study of a similar electrostatic method of alginate bead formation [37] showed that with a 23 gauge needle the minimum bead size that could be achieved varied between 600 μm and 1000 μm using a sodium alginate solution when 5 kV was applied to the capillary tip. In our studies at the same voltage and a slightly larger needle

(22 gauge) we have obtained a bead diameter 50 % smaller than that reported by Keshavarz *et al.* [37]. This difference may be partly explained by different geometry and lower viscosity of alginate solution used in our studies. With a 26 gauge needle under the same conditions the bead diameter, in our studies, decreased further, to about 150 ± 100 μm, suggesting a strong influence of needle size on bead diameter.

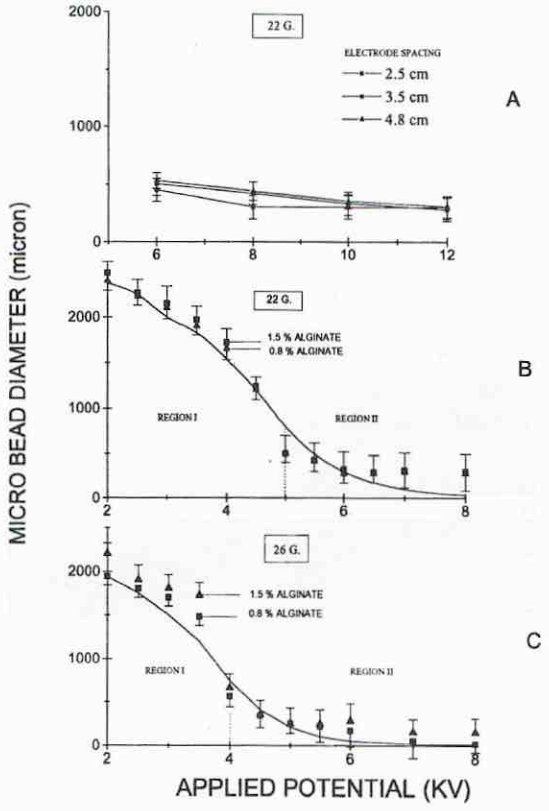

Figure 3. Effects on microbead size of A) Applied potential and electrode spacing; B) Alginate concentration and C) Needle size with the positively charged needle set-up. A 22 gauge needle was used in A) and B) and a 26 gauge needle in C).

3.2. EFFECT OF ELECTRODE GEOMETRY ON MICROBEAD SIZE

In the case of the parallel plate set-up, the effect of electrode spacing and charge arrangement (*i.e.* different electric field and surface charge intensity) on polymer bead size is shown in Figure 4A. As the potential between the electrodes in the parallel plate set-up for example, increased from 6 to 12 kV at 4.8 cm, the average bead diameter decreased from 2300 μm to 700 μm using a 22-gauge needle. Reducing the electrode distance resulted in even smaller bead sizes suggesting a strong influence of distance

and voltage on microbead size with this charge arrangement. For example, at 10 kV, reducing the distance from 4.8 cm to 2.5 cm resulted in a decrease in polymer bead diameter from 1500 μm to 350 μm. However increasing the applied potential above 12 kV and decreasing the electrode spacing did not result in further decrease in bead diameter. This was probably due to a discharge between the plates accompanied by sparking as a result of air ionization in the space between the electrodes.

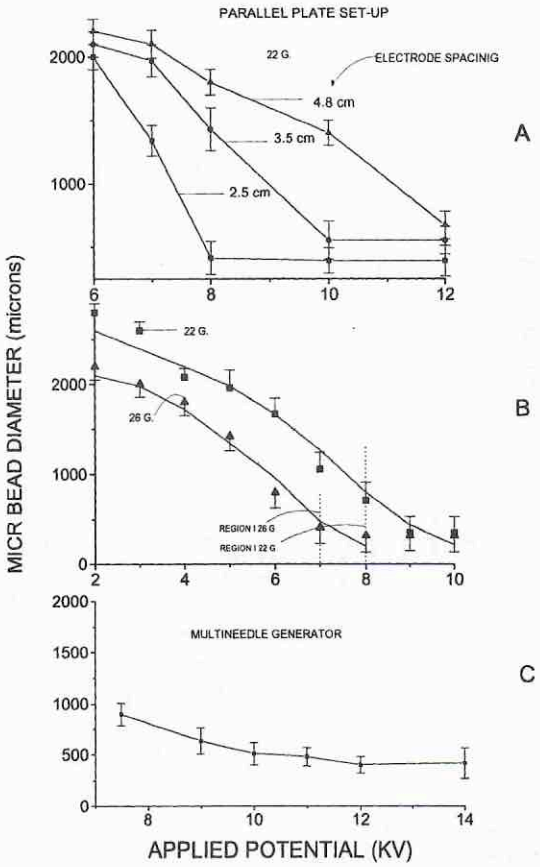

Figure 4. Effects on microbead diameter of A) Applied potential and electrode spacing, B) Needle size, and C) Scale–up with a parallel plate set-up.

For a fixed electrode distance (2.5 cm), needle length (1.3 cm) and alginate concentration (1.5%) the bead diameter could be reduced by decreasing the needle size from 22 to 26 gauge (Figure 4B). A decrease by a factor of two in bead diameter was observed for a wide range of applied potentials (2-8 kV).

The multiple needle device was essentially a scaled-up version of the parallel plate set-up (Figure 2C). Results where similar to that found with the single needle setup (Figure 2A). At an electrode distance of 2.5 cm increasing the potential from 7 to 12 kV resulted in a decrease in bead diameter from 950 μm ± 100 μm, to 400 ± 150 μm (Figure 4C). The device for the continuous beads production had a processing capacity of 0.7 L/h.

3.3. INVESTIGATION OF MECHANISM OF DROPLET FORMATION WITH IMAGE ANALYSIS/VIDEO SYSTEM

In the absence of an electrostatic field with gravitational force acting alone, the mean bead diameter was 2400 μm ± 200 μm at a constant alginate flow rate of 36 ml/h and using a 22 gauge needle. In this case a droplet was produced every one to two seconds. Each drop grew at the tip of the needle until its weight overcame the net vertical component of the surface tension force (Figure 5A).

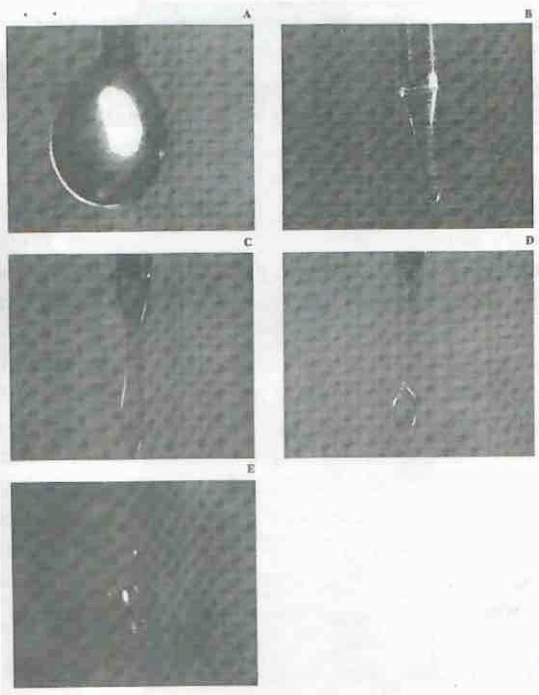

Figure 5. Electrostatic droplet formation at the needle tip with 1.5% sodium alginate without applied potential (A) and at applied potentials between 4 and 5 kV: (B) Meniscus formation; (C) Neck formation; (D) Stretching of the liquid filament; (E) Brake-up of the liquid filament.

Examination of the formation of droplets under the influence of electrostatic forces revealed that an elongated cone formed as the droplet meniscus advanced (Figure 5B). The forming droplet was drawn out into a long slender filament (voltage of 4-5 kV,

2.5 cm electrode distance, 1.5 % sodium alginate concentration, flow rate of 36 ml/h, 22 gauge needle). A high charge density at the tip of the inverted cone reduces the surface tension of the alginate solution [38] resulting in neck formation (Figure 5C). For the more concentrated alginate (*i.e.* 1.5%) we observed that the neck elongated up to one 1 mm before detachment (Figure 5D). While the main part of the liquid neck, quickly coalesced into a new drop, the long linking filament broke up into a large number of smaller drops (Figure 5E). It was also observed that small (satellite) droplet formation usually accompanied higher voltages (above 6 kV), because the elongation of the liquid neck prior to rupture was much more pronounced. The largest of these drops was one half of the main drop diameter while the smallest was less than 20 μm.

When the concentration of the alginate was decreased from 1.5% to 0.8%, a difference was observed in the formation of the long thin neck or a filament linking the new droplet and the meniscus at the tip of the needle. For the low viscosity alginate, neck elongation was not as pronounced, resulting in a more uniform bead size (Figure 6A-C).

Briefly, at the early stage, the shape of liquid meniscus is almost spherical. After the voltage is applied the meniscus is distorted into a conical shape as shown in Figure 6. Consequently the alginate solution flows through this weak area at an increasing rate causing the formation of a neck. When the filament breaks away the meniscus of the liquid on the needle is suddenly decreased for a short period until flow of the liquid causes the process to start again.

When the voltage was increased above 6 kV, harmonic natural needle oscillation was observed, but only with the thinner and lighter 26-gauge needle. A high surface charge and an electric field on the surface of capillary tip, gave rise to a mechanical force causing needle vibration and resulting in an oscillating thread-like filament (Figure 7A).

The periodic oscillation of the electrically stressed meniscus at the capillary tip caused a sinusoidal shaped filament to detach from the meniscus at the needle tip. The long tapered filaments are formed as a result of the surface energy component arising from the presence of the surface charge. From a consideration of the minimum surface energy, molecular forces tend to decrease the surface to volume ratio, whereas increasing this ratio minimizes the energy component due to electrostatic charges. Figure 7B indicates the manner in which the stream disintegrates by a vigorous whipping action. Fragmentation of the filament results in a bimodal size distribution with peaks at 50 μm and 190 μm in diameter. This phenomenon was not observed with a 22-gauge needle.

Let us examine the different mechanisms of droplet formation in regions I and II (Figure 3) for the charged needle set-up (*i.e.* Figure 2B). In the region I, the primary factor regulating droplet size is probably the intensity of the electric field in the vicinity of the forming droplet. Since the electric field increases with decreasing diameter, the intensity of the field is the highest at the meniscus tip. Formation of a continuous thin liquid filament and its break-up into small droplets is probably induced by an interaction between the surface charge on the liquid meniscus and the external electric field.

Figure 6. Droplet formation using low alginate concentration (0.8%). A) Meniscus formation; B) Filament detachment from the tip of the needle; C) Dispersion of the liquid filament.

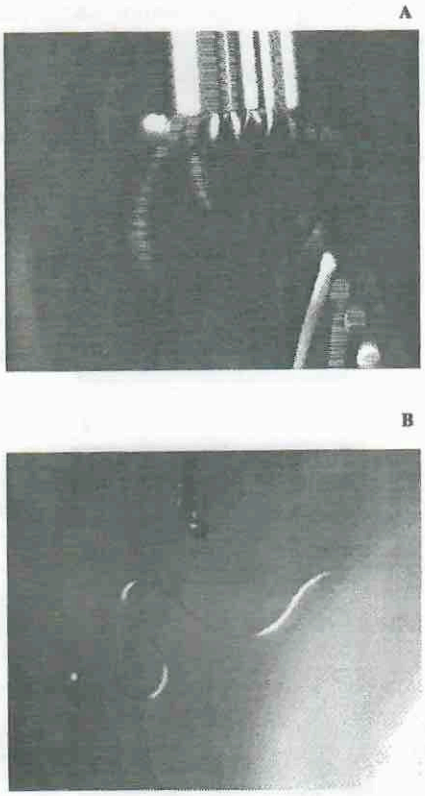

Figure 7. Needle oscillation (26 gauge, 7 kV). A) Needle vibration due to electrostatic forces, B) Detachment of liquid filament.

The electric charge on the surface of droplets gives rise to the mechanical force that is directed normally outward from the surface (*i.e.* in direct opposition to the inward acting surface forces). Also, gravity acts in the same direction as the electric field. Consequently, the terminal velocity of the charged droplet will increase. In addition, liquid surface tension may change in electric field as first proposed by Sample and Bollini [26]. They showed that the dynamic surface tension was generally higher than the static surface tension for the same liquid. For example, the surface tension of water reached a dynamic value of 0.110 N/m, as compared to a static value of only 0.074 N/m. On the other hand, distribution of the charge can take place only on the surface of the liquid so that mutual repulsion forces may cause a reduction of the surface tension. The result of these two effects (*i.e.* – increased velocity and reduced surface tension) is the increase of the Reynolds and Weber numbers of the charged droplet and the observed effect of a decrease in the droplet diameter with the increase in the electric field in region I (Figure 3).

Further increase in the voltage in region II (above 8 kV in our set-up) resulted in a slight increase in the mean bead diameter before discharge and air ionization occurred. A possible increase in surface tension in region II at higher applied potentials (> 8 kV) did not result in any further decreases in droplet diameter. Based on video/image analysis, the properties of surface charge can be used to explain the levelling off of the droplet diameter with increasing potential in region II. When a sufficiently large charge is added to the droplet, the latter may not have enough time for break-up due to the high velocity induced by the intense electric field.

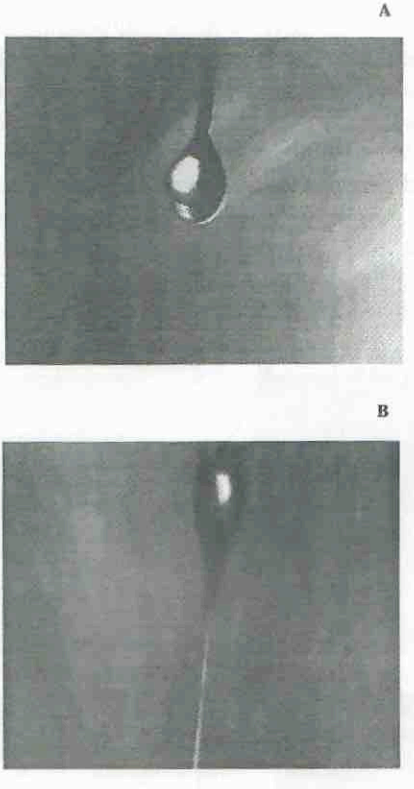

Figure 8. Comparative analysis of parallel plate and positively charged needle at the same potential (6 kV) and electrode distance (2.5 cm). A) Parallel plate set-up, B) Positively charged needle. Note the formation of the jet spray in Figure B.

A comparative analysis of the two charge set-ups (Figure 2A,B) at the same applied potential and needle size was carried out in order to give insight into the droplet formation mechanism. Looking at the formation of the droplet at the needle tip using the image analysis/video system, it was observed that each charge setup produced a different mode of droplet formation. At the same relatively high potential difference (6 kV), needle size (26 gauge), electrode spacing (2.5 cm) and flow rate (36 ml/h) there was a noticeable difference in bead diameters. With the parallel plate charge set-up, for

example, we observed that at the given potential difference, the frequency of droplets leaving the tip of the needle was below that required to initiate spraying. The average mean diameter was found to be 1100 μm ± 200 μm (Figure 8A). In contrast, with a positively charged needle a Taylor cone like meniscus [36] was observed with a well developed jet (80 μm diameter) ejecting droplets of 170 ± 70 μm in diameter (Figure 8B), a decrease by factor seven.

3.4. MICRO BEAD SIZE DISTRIBUTION

The mean bead size distribution curves obtained by plotting relative frequencies *versus* bead diameters typically resulted in a continuous function symmetrical about the mean value (Figure 9A). At 4.5 kV and 6 kV, the mean bead size distribution was found to vary about the mean of 225 μm (Figure 9A) and 170 μm (Figure 9B) respectively. However, in case of the naturally vibrating needle (7 kV), a bimodal bead size distribution was observed, one peak at 50 μm and a second peak at 190 μm (Figure 9C).

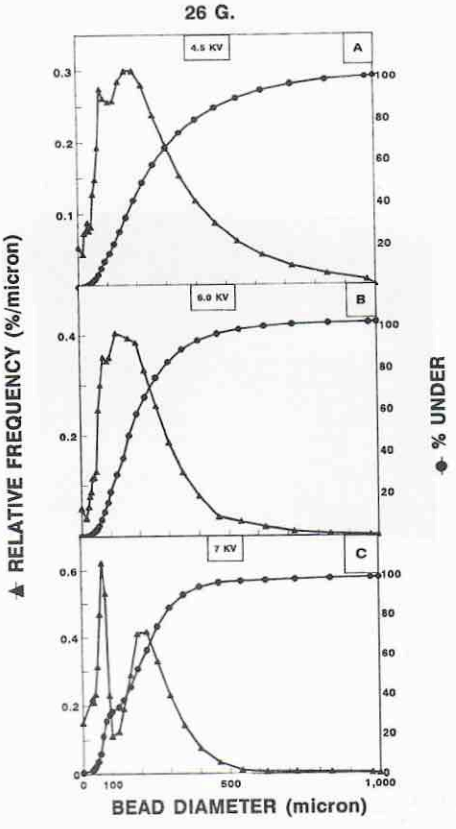

Figure 9. Droplet size distribution produced with positively charged 26 gauge needle, 2.5 cm electrode distance, 0.8% alginate concentration and electric potentials of: A) 4.5 kV, B) 6 kV, C) 7 kV.

3.5. IMMOBILIZATION OF CELLS AND ENZYMES USING ELECTROSTATIC DROPLET GENERATOR

To assess the effect of an electrostatic field on animal cells viability, an insect cell suspension was directly exposed by extrusion to the electrostatic field. No detectable change in insect cell viability was observed after extrusion. The initial cell density, 4×10^5 cell/ml, remained essentially unchanged at 3.85×10^5 cell/ml and 3.8×10^5 cell/ml immediately after passing trough the generator with an applied potential difference of 6 kV and 8 kV, respectively. Prolonged cultivation of these cells did not show any loss of cell density or viability [15].

Results of a short time cultivation study have indicated an optimal diameter range of 500 to 600 μm for alginate microbeads loaded with brewing yeast cells. When parameters of electrostatic field such as applied potential, needle size and electrode distance were adjusted a uniform beads (500 ± 50 μm) with immobilized yeast were obtained which reached a maximum cell concentration of 2.3×10^9 cell/ml bead after one week of batch cultivation (Figure 10A) [33].

Electrostatically obtained microbeads less than 150 μm in diameter, coated with poly-l-lysine were found to be effective as microcarriers for culturing surface attached insect cells, which reached a density of 1.5×10^7 cells/ml beads (Figure 10B) [28].

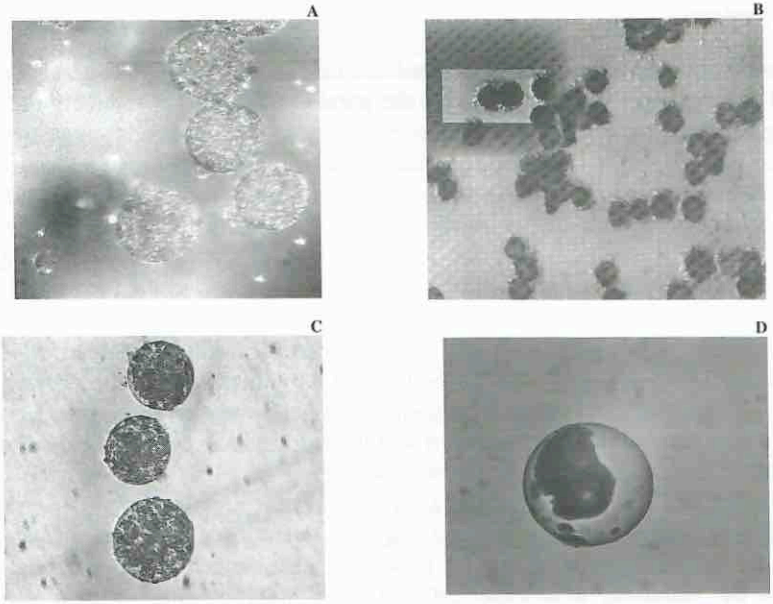

Figure 10. Different cell types immobilized using electrostatic droplet generation: A) Yeast cells, B) Insect cells/surface attachment, C) Hybridoma cells, D) Langerhans islet/single islet encapsulation.

Biological outputs such as cell density and productivity of IgG, were used to test suitability of the immobilization method and a bioreactor system for monoclonal antibody production. In this system utilising alginate-poly-l-ornithine (PLO) microcapsules (300-400 μm in diameter) cell density reached 1.5 x 10^8 cells/microcapsule, with IgG product concentration at a level of 700 μg/ml (Figure 10C) [4,27].

An artificial cell system of encapsulated islets of neonatal rat pancreas was tested for functional activities, after utilizing spraying mode to produce alginate-PLO microcapsule. Spherical microcapsules of approximately 200 μm each containing 1 islet were obtained using electrostatic field. Islets maintained functional insulin response to glucose stimulation and preserved integrity of the cell surface antigens (Figure 10D) [29,30].

Lipase from *Candida rugosa* was immobilized in alginate beads in the electrostatic field for the application in a non-aqueous reaction system. Electrostatic droplet immobilization provided monodispersed immobilized lipase alginate beads (600 μm) with negligible loss of enzyme and was proven to be more efficient in comparison to a free lipase system [39]. The beads retained high lipase activity in a reaction system of palm oil hydrolysis with the immobilization efficiency of about 99% [35].

4. Conclusions

The formation of droplets from a charged needle and a parallel plate arrangement, in a defined electric field, was examined. In the parallel plate set-up, reducing the electrode distance and increasing the applied voltage resulted in smaller beads suggesting a strong influence of distance and applied potential on bead diameter. Further reduction in bead size, with both set-ups, was achieved by decreasing the needle size. Electrode spacing was not important with the charged needle arrangement. The greatest decrease in microbead size was observed when a natural needle oscillation, caused by surface charge and a high electric field in the vicinity of the needle, resulted in whip-like liquid filaments breaking off at the end of the needle. This phenomenon produced a bimodal size distribution with a large fraction of droplets below 50 μm in diameter. Modification of the parallel plate set-up system in the form of a multi-needle device showed that it is possible to continuously produce uniform microbeads at a high processing capacity. Finally, there was no detectable loss in viability after passing animal cells through the electrostatic droplet generator. This is a promising result as it proves the technique amenable for cell immobilization. The size dispersion remains low in spraying mode [15,22,23,40]. Further experiments are required to more fully understand and control droplet formation. By combining jet formation under electrostatic potential with jet breakage by vibration, it is expected that small microcapsules with a narrow size distribution may be prepared. For laboratory applications, the present design is suitable, but it is necessary to design a pilot plant system with higher flow rates to obtain basic parameters for implementation at the industrial scale.

Acknowledgements

This work was funded by the Ministry of Science, Technologies and Development of the Republic of Serbia.

References

[1] Goosen, M.F.A.; Mahmud, E.S.C.; M-Ghafi, A.S.; M-Hajri, H.A.; Al-Sinani, Y.S. and Bugarski, M.B. (1997) Immobilization of cells using electrostatic droplet generation. In: Bickerstaff, G.F. (Ed.) Immobilization of Enzymes and Cells. Humana Press. Totowa, NJ, Chapter 20; pp. 167-174.

[2] Balchhandran, W. and Bailey, A.G. (1984) The dispersion of liquids using centrifugal and electrostatic forces. IEEE Trans. Ind. App. IA20: 682-686.

[3] Fillimore, G.L. and Lokeren, D.C. (1982) Multinozzle drop generator which produces uniform break-up of continuous jets. Institute of Electrical and Electronics Engineers, Annual Meeting of the Industrial Application Society: 991-998.

[4] Bugarski, B.; Jovanović, G. and Vunjak G. (1993) Bioreactor systems based on microencapsulated animal cell cultures. In: Goosen, M.F.A. (Ed.) Fundamentals of Animal Cell Encapsulation and Immobilization. CRC Press Inc., Boca Raton, Florida, Chapter 12; pp. 267-296.

[5] Romo, S. and Perezmartinez, C (1997) The use of immobilization in alginate beads for long-term storage of Pseudanabaena-Galeata (Cyanobacte-ria) in the laboratory. J. Phycol. 33: 1073–1076.

[6] Walsh, P.K.; Isdell, F.V.; Noone, S.M.; Odonovan. M.G. and Malone, D.M. (1996) Growth patterns of *Saccharomyces cerevisiae* microcolonies in alginate and carrageenan gel particles: effect of physical and chemical properties of gels. Enzyme Microb. Technol. 18: 366–372.

[7] Green, K.D.; Gill, I.S.; Khan, J.A. and Vulfson, E.N. (1996) Microencapsulation of yeast cells and their use as a biocatalyst in organic solvents. Biotechnol. Bioeng. 49: 535–543.

[8] Poncelet, D.; Bugarski, B.; Amsden, B.G.; Zhu, J.; Neufeld, R and Goosen, M.F.A. (1994) A parallel-plate electrostatic droplet generator: parameters affecting microbead size. Appl. Microbiol. Biotechnol. 42: 251–255.

[9] Poncelet, D.; Desmet, B.P.; Beaulieu, C.; Huguet, M.L.; Fournier, A. and Neufeld, R.J. (1995) Production of alginate beads by emulsification internal gelation. Appl. Microbiol. Biotechnol. 43: 644–650.

[10] Begin, F.; Castaigne, F. and Goulet, J. (1991) Production of alginate beads by a rotative atomizer. Biotechnol. Tech. 5: 459–464.

[11] Ogbonna, J.C.; Matsumura, M. and Kataoka, H. (1991) Effective oxygenation of immoblized cells through reduciton in bead diameter: a review. Process Biochem. 26: 109–121.

[12] Klein, J.; Stock, J. and Vorlop, K.D. (1983) Pore size and properties of spherical Ca-alginate biocatalysts. Eur. J. Appl. Microbiol. Biotechnol. 18: 86–91.

[13] Levee, M.G.; Lee, G.M.; Paek. S.H. and Palsson, B.O. (1994) Microencapsulated human bone-marrow cultures: a potential culture system for the clonal outgrowth of hematopoietic progenitor cells. Biotechnol. Bioeng. 43: 734–739.

[14] Kwok, K.K.; Groves, M.J. and Burgess, D.J. (1991) Produciton of 5–15 mm diameter alginate polylysine microcapsules by air-atomization technique. Pharm. Res. 8: 341–344.

[15] Bugarski, B.; Li, Q.L.; Goosen, M.F.A.; Poncelet, D.; Neufeld, R.J. and Vunjak, G. (1994) Electrostatic droplet generation: mechanism of polymer droplet formation. AICHE J. 40: 1026–1031.

[16] Halle, J.P.; Leblond, F.A.; Pariseau, J.F.; Jutras, P.; Brabant, M.J. and Lepage, Y. (1994) Studies on small (less than 300 mm) microcapsules. II. Parameters governing the production of alginate beads by high-voltage electro-static pulses. Cell Transplant. 3: 365–372.

[17] Prusse, U.; Fox, B.; Kirchhof, M.; Bruske, F.; Breford, J. and Vorlop, K.D. (1998) New process (jet cutting method) for the production of spherical beads from highly viscous polymer solutions. Chem. Eng. Technol. 21: 29–33.

[18] Brandenberger, H. and Widmer, F. (1997) Monodisperse particle production: a new method to prevent drop coalescence using electrostatic forces. J. Electrostat. 45: 227–238.

[19] Ghosal, S.K.; Talukdar, P. and Pal, T.K. (1993) Standardization of a newly designed vibrating capillary apparatus for the preparation of microcapsulses. Chem. Eng. Technol. 16: 395–398.

[20] Seifert, D.B. and Phillips, J.A. (1997) Production of small, monodispersed alginate beads for cell immobilization. Biotechnol. Prog. 13: 562–568.

[21] Serp, D.; Cantana, E.; Heinzen, C.; von Stockar, U. and Marison, I.W. (2000) Characterization of encapsulation device for the production of monodisperse alginate beads for cell immobilization. Biotechnol. Bioeng. 70(1): 41-53.
[22] Bugarski, B.; Amsden, B.; Neufeld, R.; Poncelet, D. and Goosen, M.F.A. (1994) Effect of electrode geometry and charge on the production of polymer micobeads by electrostatics. Can. J. Chem. Eng. 72: 517-522.
[23] Poncelet, D.; Babak, V.G; Neufeld, R.J.; Goosen, M. and Bugarski, B. (1999) Theory of elecrostatic dispersion of polymer solution in the production of microgel beds containing biocatalyst. Adv. Colloid Interface Sci. 79(2-3): 213-228.
[24] Rayleigh, Lord (1882) On the equilibrium of liquid condusting masses charged with electricity. Phil. Mag. 14: 184-186.
[25] Nawab, M.A. and Mason, S.G. (1958) The preparation of uniform emulsions by electrical dispersion. J. Colloid Sci. 13: 179-187.
[26] Sample, S.B. and Bollini, R. (1972) Production of liquid aerosols by harmonic electrical spraying. J. Colloid. Sci. 41: 185-193.
[27] Bugarski, B.; Vunjak, G. and Goosen, M.F.A. (1999) Principles of bioreactor design for encapsulated cells. In: Kuhtreiber, W.M.; Lanza, R.P. and Chick, W.L. (Eds.) Cell Encapsulation Technology and Therapeutics. Birkhauser, Boston; Chapter 30; pp. 395- 416.
[28] Bugarski, M.B.; Smith, J.; Wu, J. and Goosen, M.F.A. (1993) Methods for animal cell immobilization using electrostatic droplet generation. Biotechnol. Tech. 7(9): 677-682.
[29] Bugarski, M.B.; Sajc, L.; Plavšić, M.; Goosen, M.F.A. and Jovanović, G. (1997) Semipermeable alginate-PLO microcapsule as a bioartificial pancreas. In: Funatsu, K.; Shirai, Y. and Matsushita, T. (Eds.) Animal Cell Technology, Basic and Applied Aspects. Volume 8, Kluwer Academic Publishers, London, Boston, Dordrecht; pp. 479-486.
[30] Rosinski, S.; Lewinska, D.; Migaj, M.; Wozniewicz, B. and Werynski, A. (2002) Electrostatic microencapsulation of parathyroid cells as a tool for the investigation of cell's activity after transplantation. Landbauforschung Völkenrode SH 241: 47-50.
[31] Pjanović, R.; Goosen, M.F.A.; Nedović, V. and Bugarski, M.B. (2000) Immobilization/encapsulation of cells using electrostatic droplet generation. Minerva Biotechnology 12: 241-248.
[32] Nedović, A.V.; Obradović, B.; Leskošek, I.; Pešić, R. and Bugarski, B. (2001) Electrostatic generation of alginate microbeads loaded with brewing yeast. Process Biochem. 37: 17-22.
[33] Nedović, V.A.; Obradović, B.; Poncelet, D.; Goosen, M.F.A.; Leskošek-Čukalović, I. and Bugarski, B. (2002) Cell immobilisation by electrostatic droplet generation. Landbauforschung Volkenrode SH 241: 11-18.
[34] Knežević, Z.; Bobić, S.; Milutinović, A.; Obradović, B.; Mojović, Lj. and Bugarski, B. (2002) Alginate immobilized lipase by electrostatic extrusion. Process Biochem. 38: 313-318.
[35] Bugarski, B. and Goosen, M.F.A. (1996) Methods for animal cell immobilization using electrostatic extrusion. In: Kobayashi, T.; Kitagawa, Y. and Okumura, K. (Eds.) Animal Cell Technology, Basic and Applied Aspects. Volume 6, Kluwer Academic Publishers, London, Boston, Dordrecht; pp. 157-160.
[36] Taylor, G.I. and Van Dyke M.D. (1969) Electrically driven jets. Proc. R. Soc. A. 313: 453-475.
[37] Keshavarz, T.; Ramsden, G.; Phillips, P.; Mussenden, P. and Bucke, C. (1992) Application of electric field for production of immobilized biocatalysts. Biotech. Tech. 6: 445-450.
[38] Hendricks, C.D.Jr. (1962) Charged droplet experiments. J. Colloid Sci. 17: 249-259.
[39] Mojović, Lj.; Šiler-Marinković, S.; Kukić, G.; Bugarski, M.B. and Vunjak-Novaković, G.V. (1994) *Rhizpus arrhizus* lipase-catalyzed interesterification of palm oil midfraction in a gas-lift reactor. Enzyme Microb. Technol. 16:159-162.
[40] Poncelet, D.; Neufield, R.J.; Goosen, M.F.A.; Bugarski, M.B. and Babak, V. (1999) Formation of microgel beads by electrostatic dispersion of polymer solutions. AIChE J. 45: 2018-2023.